Conf-920768--7

High-Energy Resolution, High-Angular Acceptance Crystal Monochromator.*

ANL/XFD/CP--76595

DE93 004195

T.S. Toellner, T. Mooney and E.E. Alp
Advanced Photon Source
Argonne National Laboratory
9700 South Cass Avenue
Argonne, IL 60439

and
S. Shastri
Department of Applied Physics
Cornell University
Ithaca, New York 14853

June, 1992

cz

*This work supported by the U.S. Department of Energy, BES-Materials Sciences, under contract no. W-31-109-ENG-38

HIGH ENERGY RESOLUTION, HIGH ANGULAR ACCEPTANCE CRYSTAL MONOCHROMATOR

T. S. Toellner, T. Mooney, S. Shastri [(1)], E. E. Alp

Advanced Photon Source
Argonne National Laboratory, Argonne, Illinois, 60439
and
[(1)] *Department of Applied Physics*
Cornell University, Ithaca, New York, 14853

ABSTRACT

The design principles, construction and characterization of a 4-bounce dispersive crystal monochromator is discussed. This monochromator is designed to reduce the bandpass of synchrotron radiation to 10-50 meV level, without sacrificing angular acceptance. This is achived by combining an asymmetrically-cut, low order reflection with a symmetrically-cut, high order reflection in a nested configuration. This monochromator is being used as a beam conditioner for nuclear resonant scattering of synchrotron radiation to produce x-rays with μeV-neV resolution in the hard x-ray regime.

1. INTRODUCTION

Monochromatization of the hard x-ray component (5-30keV) of synchrotron radiation down to the ueV-neV level may be achieved via coherent nuclear resonant scattering. (1,2) This technique involves a nuclear resonant medium whose coherent response can produce an energy band-pass of μeV-to-neV. However, the nuclear resonant medium also has a non-resonant response (viz. Rayleigh scattering) which, if not suppressed, would normally overwhelm the detection system and lead to a prohibitively poor signal-to-noise ratio. Despite available techniques to suppress non-resonant scattering, it is extremely beneficial to reduce the energy bandpass of the x-ray beam as much as possible before it is incident on the nuclear resonant medium. After preliminary remarks, we present the design and testing of a high-resolution monochromator with large angular acceptance for the ^{57}Fe Moessbauer resonance (E=14.413keV). This monochromator, which is suitable for wiggler and undulator insertion devices, has a band-pass of 11 meV and an acceptance of 4.5 arcseconds.

2. APPROACH

The high brightness of undulators provide high flux in the resonant band-width ir the form of a very low-divergence beam. This low divergence (vertical divergence ≈ 5 arcsec) makes high resolution ($\Delta E/E \approx 10^{-6}$) monochromatization in the hard x-ray regime with single-crystal silicon practicable. The reason for this is essentially that the beam divergence of these insertion devices approaches the Darwin width of single-crystal reflections. As a result, one can accept an appreciable fraction of the diverging x-rays in the resonant band-width.

In order to construct such a crystal monochromator with large angular acceptance and high resolution, we shall examine the requirements for these characteristics. The energy resolution for Bragg diffraction from a perfect crystal can be approximated by $\Delta E/E \approx \Delta\theta \cot\theta_B$ where θ_B is the Bragg angle and $\Delta\theta$ is the incident divergence. From the theory of dynamical diffraction of x-rays from perfect crystals the angular acceptance for a monochromatic beam is the Darwin width, which, for symmetrically-cut crystals, is given by $\Delta\theta_s = \frac{2}{\sin 2\theta}\frac{r_e\lambda^2}{\pi V} C|F_H|e^{-M}$, where r_e= clasical electron radius, λ= wavelength, θ_B is the Bragg angle, V is the unit cell volume, C= 1 for σ-polarized radiation, $|F_H|$ is the structure factor in the scattering direction, and e^{-M} is the Debye-Waller factor.

Typically, one attempts to achieve energy resolution with large Bragg-angle reflections, since in this case $\cot(\theta_B)$ becomes small. The problem with this strategy is that the Darwin width also becomes small at higher Bragg angles (unless $\theta_B \geq 80$, where $\Delta\theta_s$ increases substantially). Thus, eventhough one can obtain very good energy resolution, the beam divergence that can be accepted is exceedingly small. To circumvent this problem one needs to reduce the beam divergence to accommodate the narrow acceptance of the higher-order reflections. This can be accomplished with the use of asymmetrically-cut crystals.

By cutting a crystal at an angle (α) with respect to the diffracting planes the angular acceptance becomes $\Delta\theta_a = \Delta\theta_s/b$, where $b = \sin(\theta_B - \alpha)/\sin(\theta_B + \alpha)$. Note that the incident x-rays and the exiting x-rays see opposite asymmetry angles. As a result, the angular acceptance of the incident x-rays will increase, while the allowed divergence of the exiting x-rays will decrease with respect to $\Delta\theta_s$. Thus, an asymmetrically-cut crystal has a collimating effect and using it in conjunction with a high-order reflection can result in high energy resolution with a much increased angular acceptance. From here, one needs to find an optimal combination of Bragg reflections, asymmetry angle, and relative orientation to achieve the desired acceptance and resolution.

For this, DuMond diagrams offer a convenient, graphic means of studying the effect of a multiple crystal-diffracting system. We produced software that creates the DuMond diagram for a specified configuration. The code, based on an algorithm by T.J.Davis (4), allowed us to examine the performance of a number of possible configurations before settling on an actual design.

3. DESIGN

For the design we chose a silicon (10 6 4) channel-cut nested within an asymmetrically-cut (α=20) silicon (4 2 2) channel-cut to form a (+m,+n,-n,-m) dispersive geometry (fig.1). This design, initially proposed by Ishikawa, et al.(5), produces an incident angular acceptance of 4.5" and an energy band-pass of 11.7meV.

Our choice for the asymmetry angle that produces this angular acceptance, was based on a number of criteria. Although angular acceptance was the main concern, we also considered the required alignment between the two channel-cuts (c.c.), the effect of too large an asymmetry angle, as well as the overall size of the monochromator. The required alignment between the c.c. is dictated by the exiting divergence of the first face

and the Darwin width of the second face (i.e.the (10 6 4)). So the result here is that a larger asymmetry angle forces a more restrictive rotational alignment. Large asymmetry angles have another side-effect. As $|\alpha|$ approaches θ_B the incident beam becomes glancing and the amount of losses due to diffuse scattering from a rough surface increases. To avoid this, we wanted $\theta - |\alpha| > 2$. Also, as the asymmetry angle increases, the size of the diffracted beam increases as $S_{Diff} = S_{Inc}/b$ As a result, the nested c.c. must be made larger to accomodate the diffracted beam and, this, in turn, increases the overall size of the monochromator. Our choice of asymmetry angle reflects a consideration of all these effects. The result is depicted graphically in the DuMond diagram of fig.2. From a transformation of this DuMond plot into the coordinates of the beam incident on the second face, we calculated the required rotational alignment between the two crystals to be .34 arc seconds. To put a beam of the correct energy through the crystal pair, one wants angular resolution and stability of a factor of five or so better than this figure.

The monochromator is built around a pair of piezo-inchworm-driven rotation stages (Burleigh model RS-75) with angular resolutions of roughly .02 arc seconds, each coupled to an angle encoder (Heidenhain model ROD-800) with an angular resolution of .036 arc seconds and an accuracy of, perhaps, 0.5 arc seconds. In addition to problems of creep, hysteresis, and the cumulative nature of stepping irregularities in the motion of an inchworm, the effects on the Bragg angles due to variations in monochromator-crystal temperature are not ignorable. For these reasons, the inchworms are controlled dynamically by software feedback, using angle information from the encoders and temperature information from a pair of precision thermistors in thermal contact with the crystals.

Given adequate feedback control, the performance of this design depends critically on mechanical control over three sources of error in the relative angular orientation of the monochromator crystals: the relative orientation of the angle encoders, the precision of those encoders, and the coupling between the crystals and the encoders. To minimize relative motion of the encoders, the monochromator chassis is constructed entirely of stainless steel, welded into a single piece, stress relieved by heat treatment, and mounted on a vibration-isolated table. The other two sources are interdependent: encoder precision depends in part on the degree to which the encoder shaft is isolated from external forces, and the flexible coupling that can accomplish that isolation can also introduce hysteresis (shaft windup) in the crystal-encoder connection. In our current design, that connection is made with an Heidenhain model K-15 rotational coupler.

4. PERFORMANCE TESTING

To characterize the performance of the monchromator we used the 24-pole wiggler on the F-2 beamline at the Cornell High Energy Synchrotron Source (CHESS). X-rays from the wiggler were apertured to 6.3 arc seconds vertical divergence before impinging on a water-cooled silicon (111) heat-load monochromator to bring the energy band-pass down to ~5eV. From here the beam passes through the high-resolution monochromator before impinging on the nuclear resonant medium, an ^{57}Fe enriched Yttrium Iron Garnet (YIG) crystal. Finally, the diffracted beam from the YIG crystal was measured with a fast coincidence detector. See figure 4 for a picture of this set-up.

Due to the long lifetime, t=98ns, of the 14.413keV resonance in ^{57}Fe when compared to the scattering time for the non-resonant radiation it is possible to time filter the delayed resonant photons from the prompt nonresonant photons. This can be achieved as long as the nonresonant scattering does not saturate the detector. In order to insure this, we used the YIG(002) reflection that is nuclear-allowed but electronically forbidden to suppress the non-resonant radiation by a factor of 10^6 or so. From this we were able to obtain a time spectrum without the high-resolution monochromator(cf. fig.5) Note the enormous prompt peak despite the six orders-of-magnitude suppression induced by the electronically forbidden reflection.

After positioning the monochromator in the beam, a comparison of ionization chamber #1 to #2 demonstrated that the non-resonant count rate decreased by a factor of ~500 while the resonant count rate went from ~20 cps to ~2 cps. This represents a factor of ten loss in resonant count rate while reflectivity considerations only allow for a factor of two. We suspect this extra factor of five loss in resonant count rate was due to crystal misalignments, both absolute and relative, resulting from incomplete software feedback control. Note from figure 5 that the supppresion induced by the monochromator allowed the detector to regain half of the lost resonant, time response.

We used the highly monochromatic ($\Delta E/E \approx 10^{-11}$), delayed photons to characterize the energy resolution of the monochromator. To measure the energy band-pass we placed the (10 6 4) c.c. in position and collected resonant quanta as a function of its rocking angle with the (422) c.c. remaining fixed. This produced the rocking curve shown in figure 6 and from it one obtains a FWHM of 0.7±.1 arc seconds. Transforming this measured FWHM into energy coordinates results in an energy FWHM of 10.8(±1.6)meV. Of course, the full energy band-width will be slightly larger than this. The theoretical simulation of this rocking curve involved dispersively convolving the square of the exiting Darwin-Prins curve for the asymmetrically-cut (422) c.c. with that of the symmetrically-cut (10 6 4) c.c.. From this we obtained a theoretical FWHM of 0.59 arc seconds.

5. CONCLUSION

In summary, we have constructed and tested the design of a high resolution monochromator for the ^{57}Fe Moessbauer resonance at 14.413keV. The future developement of this monochromator will involve: 1) siton polishing to avoid losses due to surface roughness, 2) more complete software feedback control, and 3) constructing larger crystals to accomodate higher asymmetry angles. Also in progress, is a monochromator for the Sn-119 Moessbauer resonance at 23.87keV. This monochromator is of a similar design but, due to the higher energy, it's theoretical angular acceptance is reduced to ~2 arc seconds and it's bandpass to~40 meV.

6. ACKNOWLEDGEMENTS

We would like to thank A. M. Macrander for his assistance during the testing of the monochromator. For the use of the YIG crystal, without which the testing would have been excruciating, we would like to thank J. Arthur, G. Brown, and S. Ruby of SSRL. This work is supported by U.S. DOE, BES-Materials Sciences, under contract W-31-109-ENG-38.

7. FIGURES

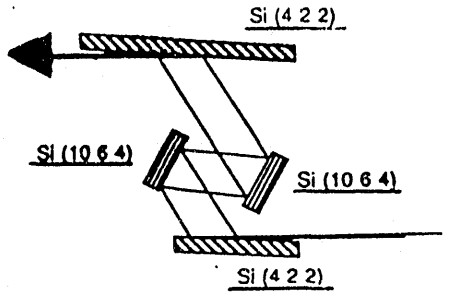

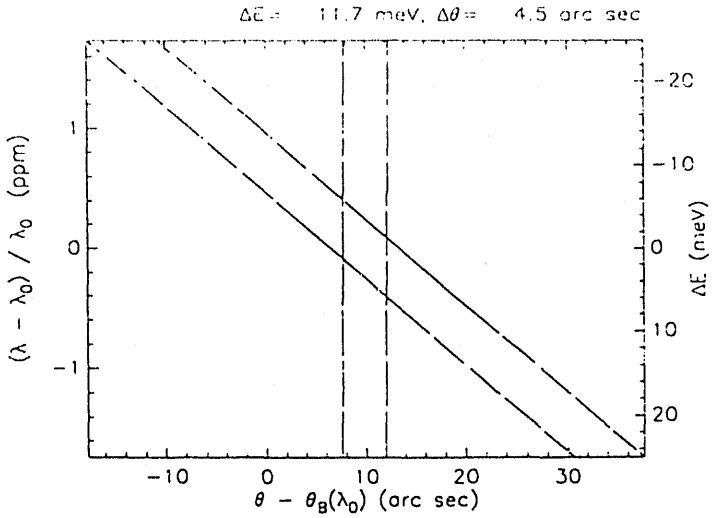

Fig. 1. Orientation of channel cuts. Note that the Si (10 6 4) crystal is nested within the asymmetrically-cut Si (4 2 2) crystal and is arranged dispersively. **Fig. 2.** The associated DuMond diagram for the crystal arrangement of figure (1) at E=14.413keV.

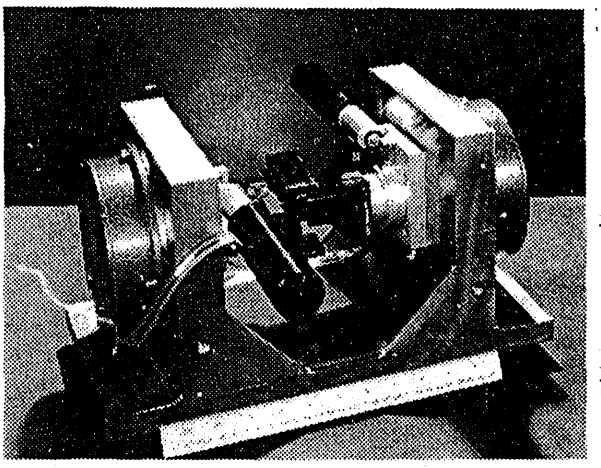

Fig. 3. Monochromator. Mounting assembly with crystals.

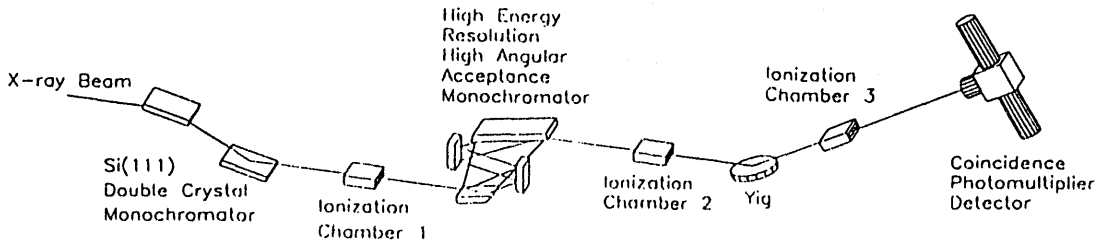

Fig. 4. Set-up to test performance of high-resolution monochromator.

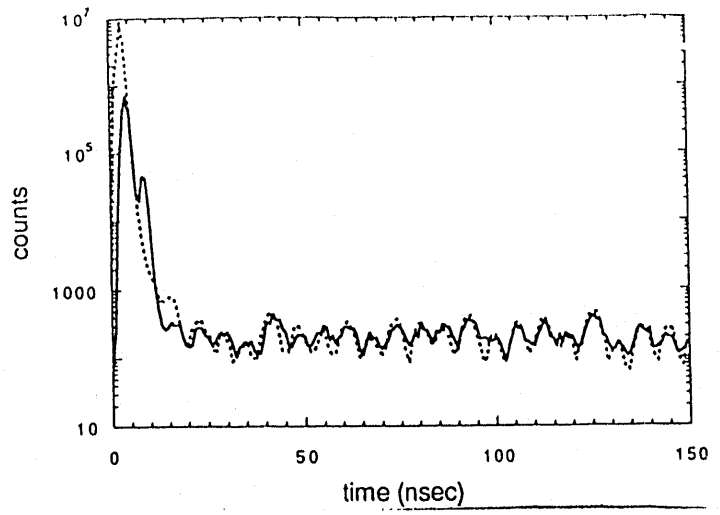

Fig. 5. Resonant time-response of YIG (002) reflection at E=14.413keV. The peak at early times (prompt peak) is due to nonresonant scattering in the YIG crystal. The oscillations are the result of coherent excitation of the nuclear hyperfine levels. Note the additional time response that is detectable after the introduction of the high resolution monochromator (dashed line). Data is normalized with respect to total integrated delayed counts.

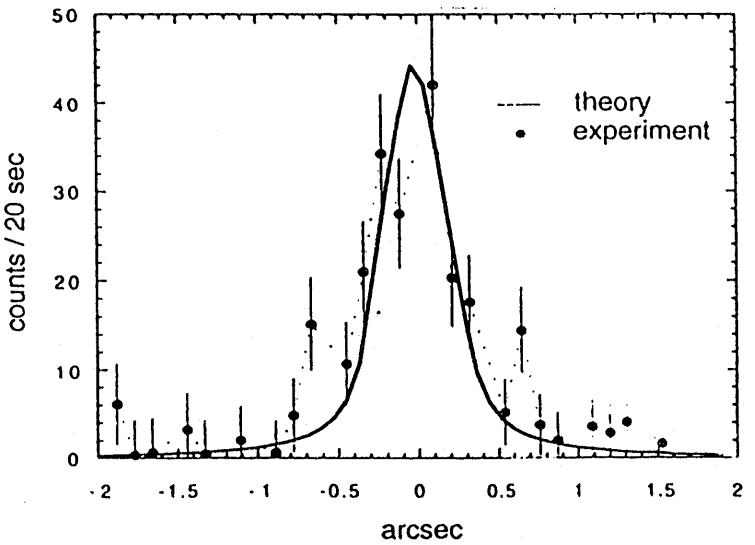

Fig. 6. Rocking curve of Si (10 6 4) against asymmetrically-cut Si (4 2 2). Measured using Moessbauer (14.413keV) photons.

8. REFERENCES

1. S. Ruby, J. Phys. (Paris), Colloq. 35, C6-209 (1974).....
2. E. Gerdau, R. Ruffer, H. Winklér, W. Tolksdorf, C.P. Klages, J.P. Hannon, Phys. Rev. Lett. **54**, 835 (1985).....
3. D.P. Siddons., J.P. Hastings, G. Faigel, J.R. Grover, P.E. Haustein, L.E. Berman, Rev. Sci. Instr. **60**, 1649 (1989).....
4. T.J. Davis, J. Sci. Tech. **2**, 180 (1990).....
5. T. Ishikawa, Y.Yoda, K. Izumi, C.K. Suzuki, X.W. Zhang, M. Ando, S. Kikuta, Rev. Sci. Instr. **63**, 1015 (1992).

DATE
FILMED
01/20/93